IEICE TRANS. INF. & SYST., VOL.E83–D, NO.8 AUGUST 2000

PAPER

A Multiple View 3D Registration Algorithm with Statistical Error Modeling*

John WILLIAMS† *and* **Mohammed BENNAMOUN**†, *Nonmembers*

SUMMARY The contribution of the paper is two-fold: Firstly, a review of the point set registration literature is given, and secondly, a novel covariance weighted least squares formulation of the multiple view point set registration problem is presented. Point data for surface registration is commonly obtained by non-contact, 3D surface sensors such as scanning laser range finders or structured light systems. Our formulation allows the specification of anisotropic and heteroscedastic (point dependent) 3D noise distributions for each measured point. In contrast, previous algorithms have generally assumed an isotropic sensor noise model, which cannot accurately describe the sensor noise characteristics. For cases where the point measurements are heteroscedastically and anisotropically distributed, registration results obtained with the proposed method show improved accuracy over those produced by an unweighted least squares formulation. Results are presented for both synthetic and real data sets to demonstrate the accuracy and effectiveness of the proposed technique.

key words: *3D registration, multiple view, anisotropic, heteroscedastic, sensor noise*

1. Introduction

The task of registering three dimensional data sets with rigid motions is a fundamental problem in computer vision, arising whenever two or more 3D data sets must be aligned in a common coordinate system. The registration problem is comprised of two related sub-problems: correspondence selection and motion estimation. In the former, candidate correspondences between data sets are chosen, while in the latter, rigid motions minimising the distances between corresponding points are estimated. Space limitations prevent in-depth discussion of both, and in this paper we focus upon the motion estimation task.

An early application from the photogrammetry community is the problem of determining absolute orientation of stereo imagery. Fixed, surveyed ground control points visible in the images are used to establish a coordinate system allowing the subsequent development of topographic maps and ortho-imagery.

A more recent application is object reconstruction and reverse engineering, where multiple 3D surface scans of objects are combined to construct a complete surface model. Individual scans cover only a portion of the object surface, and registration is necessary to find the optimal alignment prior to reconstructing the surface model.

3D registration also has application in medical image analysis. Accurate measurement of biomorphological phenomena such as tumor growth is assisted by registering 3D images taken in a time sequence. In a similar fashion, multimodal images can be registered to fuse complementary data sets, providing more comprehensive diagnostic information and aiding surgical planning.

In this paper we trace the history of the 3D point set registration problem, from the photogrammetry literature of the 1960s to the modern field of computer vision. We distinguish between two specific classes of registration algorithm, and discuss desirable properties of a registration technique. In the second part of the paper, we present a novel WLSQ (weighted least squares) formulation of the registration problem, with advantages not previously found in any single algorithm.

There are two major issues which must be considered when discussing registration algorithms. The first is the distinction between pairwise and global registration methods, and the second is the treatment of errors and uncertainty. Techniques reviewed in this paper will be considered in the light of the following definitions and capabilities.

As the name suggests, pairwise registration algorithms register just two data sets at a time. Global techniques, on the other hand, perform the registration across multiple (more than two) data sets simultaneously. A pairwise technique may still be used to solve a global problem, by taking the multiple data sets two at a time, however this is not an optimal solution. In the pairwise case, an uneven distribution of registration inaccuracy can result, whereby individual pairs have high registration accuracy, yet the whole registered system may be significantly different from the truth. Truly global methods distribute registration errors evenly through the data sets. When applied to a registration problem with just two data sets, global algorithms generally reduce to an existing pairwise method.

The treatment of measurement errors is another

Manuscript received July 27, 1999.
Manuscript revised February 21, 2000.

†The authors are with the Space Centre for Satellite Navigation, School of Electrical & Electronic Systems Engineering, Queensland University of Technology, Brisbane, Australia.

*This work is based on an invited paper presented at the IEEE International Conference on Systems Man and Cybernetics (SMC '99), October 1999.

key point to consider for registration problems. In most practical applications, point positions are derived through analysis of real measurement data, however this data will be unavoidably corrupted by errors such as random measurement noise. If the statistical properties of this noise can be estimated or modeled, then it is desirable to utilise this information to improve accuracy. Due to the nature of 3D sensors, point error distributions are usually heteroscedastic (point dependent), and anisotropic [18], [20].

A related issue is performance evaluation, such as computing confidence intervals for the estimated rigid motions. Realistic measures of registration accuracy are of great value by quantifying the limits of precision available based upon the data provided.

Another source of error for registration algorithms is the correspondence selection process itself [14]. Erroneous correspondences cause significant problems, particularly for algorithms based on LSQ type optimisation. Robustness against these outliers is valuable for practical applications using real data.

The structure of the paper is as follows. Section 2 presents a review of the point set registration problem, which highlights the need for a multiple view registration scheme supporting individual point error models. This is followed by a brief description of preliminary concepts including motion representation and probabilistic point features. Section 4 then describes the problem mathematically, and introduces the notation, before the problem is formulated as a weighted least squares estimation task in Sect. 5. The solution to problem is then presented in Sect. 6, followed by a discussion of estimating motion parameter uncertainty in Sect. 7. In Sect. 8 we present results obtained from tests with both synthetic and real data, and finally our conclusions are presented in Sect. 9.

2. A Review of Point Set Registration Techniques

We present a brief review of the history of point set registration algorithms. The early work comes mostly from the photogrammetry literature, while recent efforts are dominated by researchers in the computer vision field.

Thompson [28] presented a solution to the problem of computing a scale and rotation matrix fitting exactly 3 pairs of corresponding points. A subsequent refinement and extension was proposed by Schut [25] using unit quaternions. Both of these methods were based upon Cayley's formulation for a rotation matrix $\boldsymbol{R} = (\boldsymbol{I} + \boldsymbol{S})(\boldsymbol{I} - \boldsymbol{S}^{-1})$ where $\boldsymbol{I}$ is the identity matrix and $\boldsymbol{S}$ is skew-symmetric (e.g. [29]).

These methods had several drawbacks, such as the rotation value depending upon the ordering of the points, and the scale factor being dependent upon which of the two data sets was considered the "image" of the other. They were also unable to handle cases in which the rotation was an angle of π radians about any axis [29].

Tienstra [29] formulated a constrained LSQ solution, permitting "best-fit" transformation estimates computed from more than three correspondences. A solution with similar properties was formulated using unit quaternions by Sanso [23]. Blais gives yet another approach to the problem, with the restriction that reflections, and rotations of π radians are avoided [7].

Interestingly, the pairwise registration problem is equivalent to a problem arising in psychological statistics known as the orthogonal Procrustes problem. See, for example [10], [24].

In response to problems faced by researchers in the fields of robotics and computer vision, the registration problem was "rediscovered" in the 1980s. Several of these effectively duplicated the earlier work of Tienstra and Sanso.

Closed-form solutions to the pairwise problem were proposed independently by Arun et al. [1], Horn [15], Horn et al. [16] and Haralick et al. [14]. None of these algorithms support the use of statistical point error models, however individual point contributions can be weighted based upon suspected noise levels within the data. Zhang [33], and Dorai et al. [9] propose methods for computing the weight factors based upon noisy range image data.

These closed-form, pairwise techniques are theoretically equivalent, and differ mostly through the way the problem is formulated. A recent experimental comparison found that for practical applications with non-degenerate data the differences were negligible [12]. Pennec and Thirion [22] presented a systematic treatment of data errors in the pairwise registration problem. Based upon the framework for uncertain geometric computations by Ayache [2], an iterated extended Kalman filter (IEKF) was used to compute registration parameters for point sets with heteroscedastic error distributions. Estimates of the motion parameter uncertainty were computed in the form of error covariance matrices.

Ohta and Kanatani [20] recently proposed an iterative solution to pairwise registration using renormalisation. The method supports heteroscedastic point errors, and estimates the reliability of the result through theoretical and bootstrap analysis. Matei and Meer [18] have also presented a technique with similar capabilities, based upon a multivariate errors-in-variables (EIV) regression framework. Bootstrap analysis was also used to estimate registration confidence.

Stoddart and Hilton [27] proposed the first truly global registration algorithm, which modeled views as rigid bodies, and the point correspondences as zero-length springs. Equations of classical rigid-body mechanics were then used to iteratively solve for the equilibrium positions and orientations. A similar approach was also proposed by Eggert et al. [11]. Neither ap-

proach modeled nor accounted for statistical point errors.

Benjemaa and Schmitt [4] generalised aspects of Horn's quaternion algorithm [15] to develop an iterative solution to the global registration problem. Once again point errors were not considered. Another quaternion based multiview technique was proposed by Shum et al. [26], however this work was cast within a system for simultaneous registration and reconstruction of polyhedral object models, and did not deal specifically with the problem of point set registration.

Next we consider attempts at robustness against outlier data. A number of authors have attempted to make the registration process robust against outlier data such as false correspondences. These efforts have generally utilised variants of the robust estimators described by, for example, Meer [19].

Zhang [33] and Pennec and Thirion [22] attempted to reject outliers by thresholding against a Mahalonobis distance criterion, which is based upon the assumption of a contaminated Gaussian error distribution. This is functionally equivalent to a robust M-estimator with a binary weight function.

Boulanger [8] employed a Least Median of Squares (LMedS) estimator, which is theoretically robust against up to 50% outliers. A drawback to LMedS is its low Gaussian efficiency [19], however this effect can be minimised by following the LMedS with several iterations of an appropriate robust M-estimator. Zhuang and Huang have also tackled the robust registration problem [34].

From this review, the absence of a technique supporting both global registration problems and heteroscedastic, anisotropic errors is clear. This would represent the most general class of registration algorithms, capable of solving any of the problems addressed by the preceding methods. In the next part of this paper, we present such an algorithm. The technique presented does not address robustness issues explicitly, however the reader is referred to [31] where a robust variant of this algorithm is described.

3. Preliminaries

This paper utilises concepts from the framework for probabilistic points and motions, described in [22]. The following material describes the notation used to formulate the point registration task as a constrained weighted least squares problem.

3.1 Representation of Motions

A rigid transformation $\boldsymbol{p}' = \boldsymbol{R}\boldsymbol{p} + \boldsymbol{t}$ of a point $\boldsymbol{p}$, where $\boldsymbol{R}$ a rotation matrix and $\boldsymbol{t}$ is a translation vector, can be represented a single vector $\boldsymbol{f} = (\boldsymbol{r}, \boldsymbol{t})$. The rotational $\boldsymbol{R}$ represents a rotation of angle θ around the axis specified by unit vector $\boldsymbol{n}$. By defining $\boldsymbol{r} = \theta\boldsymbol{n}$, the coordinate transformation may be represented by the 6-element vector $\boldsymbol{f} = (\boldsymbol{r}, \boldsymbol{t})$. The axis-angle and rotation matrix representations are related by Rodrigues' formula:

$$\boldsymbol{r} = \boldsymbol{I}_3 + \sin\theta\ \boldsymbol{S}_n + (1 - \cos\theta)\boldsymbol{S}_n^2$$

where $\boldsymbol{S}_n$ is the skew matrix corresponding to the left cross product ($\boldsymbol{S}_n\boldsymbol{v} = \boldsymbol{n} \times \boldsymbol{v}$, $\forall \boldsymbol{v} \in \mathbb{R}^3$) [22].

Rigid motions may be inverted, composed and applied to points. These operations are described as:

$$\begin{aligned}
&\text{Apply } \boldsymbol{f} \text{ to point } \boldsymbol{p} : \boldsymbol{p}' = \boldsymbol{f} \star \boldsymbol{p} = \boldsymbol{r} \star \boldsymbol{p} + \boldsymbol{t},\\
&\text{Invert } \boldsymbol{f} : \boldsymbol{f}^{(-1)} = (\boldsymbol{r}^{(-1)}, \boldsymbol{r}^{(-1)} \star \boldsymbol{t}),\\
&\text{Compose } \boldsymbol{f}_1 \text{ and } \boldsymbol{f}_2 : \boldsymbol{f} = \boldsymbol{f}_2 \circ \boldsymbol{f}_1\\
&\qquad\qquad = (\boldsymbol{r}_2 \circ \boldsymbol{r}_1, \boldsymbol{r}_2 \star \boldsymbol{t}_1 + \boldsymbol{t}_2).
\end{aligned}$$

3.2 Probabilistic Points

Measured point locations/ranges are corrupted by random errors or noise. Here, an additive error model is assumed for the measured point $\boldsymbol{p}$,

$$\boldsymbol{p} = \tilde{\boldsymbol{p}} + \boldsymbol{e}_{\boldsymbol{p}}$$

where $\tilde{\boldsymbol{p}}$ is the true point location (the actual physical location of the point on the object which is being sensed) and $\boldsymbol{e}_{\boldsymbol{p}}$ is a random variable characterising the measurement noise. The expected value $\mathrm{E}[\boldsymbol{e}_{\boldsymbol{p}}]$ is assumed to be zero.

The type of probability distribution, to which $\boldsymbol{e}_{\boldsymbol{p}}$ belongs, depends largely on the sensor. However, for computational reasons it is common to consider only its second order central moment (covariance matrix) [22], calculated according to

$$\boldsymbol{\Sigma}_{\boldsymbol{pp}} = \mathrm{E}\left[\boldsymbol{e}_{\boldsymbol{p}}\, \boldsymbol{e}_{\boldsymbol{p}}{}^{\top}\right]$$

where the $^{\top}$ symbol denotes matrix transpose operator. Thus, a probabilistic point may be represented by the pair $(\boldsymbol{p}, \boldsymbol{\Sigma}_{\boldsymbol{pp}})$ which indicates an expected value of the true point position $\tilde{\boldsymbol{p}}$, and the likely deviation around that position (for exact or deterministic points we simply use $\boldsymbol{\Sigma}_{\boldsymbol{pp}} = \boldsymbol{0}$). A two dimensional example of the sensor model is illustrated in Fig. 1, where the action of a scanning range finder is simulated. The range error variance is greater than that of the directional (azimuth) errors, indicating that the confidence

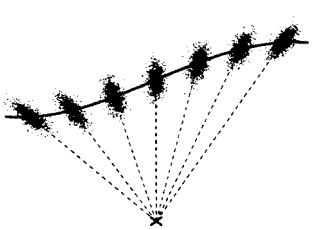

Fig. 1 Monte Carlo simulation of a range sensor with error distribution aligned with the line of sight from the sensor origin (X) to the surface (solid line).

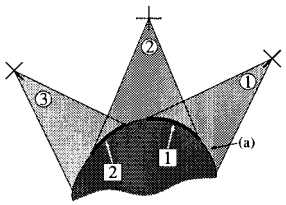

Fig. 2 Illustration of views and correspondence sets. See the text for details.

curves are approximately elliptical, with the major axis aligned with the line of sight from the sensor origin to the surface. In 3D, the ellipses become ellipsoids.

4. Problem Description

Assume the existence of M overlapping views, with their associated local coordinate systems represented by $\boldsymbol{f}^m$, $m = 1, \ldots, M$. Between the overlapping views, there exist P sets of pairwise correspondences, with $\mu = 1, \ldots, P$ indexing these sets. The mappings $\alpha(\mu)$ and $\beta(\mu)$ define the two views which participate in the μth correspondence, and let the N_μ denote the number of corresponding point pairs in each set.

Figure 2 illustrates these definitions. It depicts the partial covering of an object's surface by three views, numbered 1 to 3 (in the circles), with crosses representing the local sensor coordinate systems. The fields of view for each sensor are shown. The correspondence sets (numbered 1 and 2 in boxes) are represented by the heavy lines in the overlapping fields of view. Thus, in this case we have $M = 3$, and $P = 2$. Correspondence set $\mu = 1$ is common to views $\alpha(1) = 1$ and $\beta(1) = 2$, and set $\mu = 2$ is shared by views $\alpha(2) = 2$ and $\beta(2) = 3$. Note that points appearing in only one view – such as those in region (a) in the figure – *play no part* in the registration process.

For correspondence set μ, let the points $\boldsymbol{p}_{i,\mu}^{\alpha(\mu)}$, measured from view $\alpha(\mu)$ correspond to the points $\boldsymbol{p}_{i,\mu}^{\beta(\mu)}$ measured from view $\beta(\mu)$, $i = 1 \ldots N_\mu$. The points $\boldsymbol{p}_{i,\mu}^{\alpha(\mu)}$ and $\boldsymbol{p}_{i,\mu}^{\beta(\mu)}$ are probabilistic in the sense of Sect. 3.2, with covariance matrices denoted $\boldsymbol{\Sigma}_{i,\mu}^{\alpha(\mu)}$ and $\boldsymbol{\Sigma}_{i,\mu}^{\beta(\mu)}$, respectively.

5. Problem Formulation

The aim of the registration process is to compute a transformation for each view which, when applied to the points in that view, maximises the co-incidence of each corresponding point pair. View number 1 is chosen arbitrarily to be fixed to the canonical coordinate system and hence is not included in the estimation process. Otherwise, the system will exhibit a global degeneracy, since the same transformation applied to all views causes no improvement in the registration.

The required transformations are contained in vectors $\boldsymbol{f}^2, \boldsymbol{f}^3, \ldots \boldsymbol{f}^M$ which are concatenated into a single vector

$$\boldsymbol{\theta}^\top = \begin{bmatrix} \boldsymbol{f}^{2\top} & \ldots & \boldsymbol{f}^{M\top} \end{bmatrix}$$

As a notational convenience, the correspondence index μ shall be omitted from super/sub scripts, so that $\boldsymbol{p}_{i,\mu}^{\alpha(\mu)} \equiv \boldsymbol{p}_i^\alpha$, $\boldsymbol{p}_{i,\mu}^{\beta(\mu)} \equiv \boldsymbol{p}_i^\beta$, $\boldsymbol{\Sigma}_{i,\mu}^{\alpha(\mu)} \equiv \boldsymbol{\Sigma}_i^\alpha$ and $\boldsymbol{\Sigma}_{i,\mu}^{\beta(\mu)} \equiv \boldsymbol{\Sigma}_i^\beta$. The implicit value of the correspondence index μ should be clear from the context.

Each pair of corresponding points is combined into a single vector representation, and analogously for their covariances:

$$\boldsymbol{w}_i^\mu \equiv \begin{bmatrix} \boldsymbol{p}_i^\alpha \\ \boldsymbol{p}_i^\beta \end{bmatrix}$$

$$\boldsymbol{V}_i^\mu \equiv \begin{bmatrix} \boldsymbol{\Sigma}_i^\alpha & \boldsymbol{0} \\ \boldsymbol{0} & \boldsymbol{\Sigma}_i^\beta \end{bmatrix}$$

Thus, $\boldsymbol{w}_i^\mu = \tilde{\boldsymbol{w}}_i^\mu + \boldsymbol{e}_i^\mu$, where $\mathrm{E}[\boldsymbol{e}_i^\mu] = \boldsymbol{0}$ and $\mathrm{E}\left[\boldsymbol{e}_i^\mu \boldsymbol{e}_i^{\mu\top}\right] = \boldsymbol{V}_i^\mu$. Denoting true, but unknown, values of parameters with a tilde (e.g. $\tilde{\boldsymbol{w}}_i^\mu$), the 3D registration problem is now formulated in the form of an "exact structural model" problem [3]. This formulation is analogous to constrained WLSQ parameter estimation.

The registration problem constrains that the true points $\tilde{\boldsymbol{p}}_i^\alpha$ and $\tilde{\boldsymbol{p}}_i^\beta$ coincide when transformed into the world coordinate system. This constraint is expressed as

$$\boldsymbol{g}(\tilde{\boldsymbol{w}}_i^\mu, \tilde{\boldsymbol{\theta}}) \equiv \tilde{\boldsymbol{f}}^\alpha \star \tilde{\boldsymbol{p}}_i^\alpha - \tilde{\boldsymbol{f}}^\beta \star \tilde{\boldsymbol{p}}_i^\beta = \boldsymbol{0} \tag{1}$$

for $\mu = 1 \ldots P$, $i = 1 \ldots N_\mu$, or alternatively

$$\boldsymbol{G}(\tilde{\boldsymbol{W}}, \tilde{\boldsymbol{\theta}}) = \boldsymbol{0} \tag{2}$$

where $\boldsymbol{G}$ and $\tilde{\boldsymbol{W}}$ represent the concatenation, into column vectors, of the $\boldsymbol{g}(\tilde{\boldsymbol{w}}_i^\mu, \boldsymbol{\theta})$ and $\tilde{\boldsymbol{w}}_i^\mu$ respectively. Obviously, the true point measurements are unknown, and the aim is to seek *estimates* of the true point locations. Let the hatted quantities $\hat{\boldsymbol{W}}$ and $\hat{\boldsymbol{\theta}}$ denote the estimates of the true quantities $\tilde{\boldsymbol{W}}$ and $\tilde{\boldsymbol{\theta}}$, respectively. The estimates are subject to the same coincidence constraint (Eq. (2)) as the true values, $\boldsymbol{G}(\hat{\boldsymbol{W}}, \hat{\boldsymbol{\theta}}) = \boldsymbol{0}$.

The point measurements are considered the independent data in the estimation problem, and the residuals are defined to be the difference between the measurements and their estimated true values [3]:

$$\boldsymbol{e}_i^\mu = \boldsymbol{w}_i^\mu - \hat{\boldsymbol{w}}_i^\mu \tag{3}$$

This formulation is different to that conventionally applied to point set registration problems, and the reader is encouraged to consult [3] for more details regarding the use of exact structural models in parameter estimation problems.

By assuming that the measurement errors $\boldsymbol{e}_i^\mu$

are independently, normally distributed, the maximum likelihood estimation procedure for determining $\hat{\boldsymbol{\theta}}$ is:

Find $\hat{\boldsymbol{W}}$ and $\hat{\boldsymbol{\theta}}$, which minimise

$$\Phi(\hat{\boldsymbol{W}}) = \sum_{\mu=1}^{P}\sum_{i=1}^{N_\mu} (\boldsymbol{w}_i^\mu - \hat{\boldsymbol{w}}_i^\mu)^\top (\boldsymbol{V}_i^\mu)^{-1} (\boldsymbol{w}_i^\mu - \hat{\boldsymbol{w}}_i^\mu) \quad (4)$$

subject to $\boldsymbol{G}(\hat{\boldsymbol{W}}, \hat{\boldsymbol{\theta}}) = \boldsymbol{0}$.

Standard numerical iterative techniques can be used to obtain solutions to this constrained optimization problem. The experimental results, presented in Sect. 8, were obtained by using the method of Lagrange multipliers to incorporate the constraint into a new objective function. Newton iteration is then used to mimimise this new objective function. A benefit arising, from the use of the Newton iterative scheme, is that the derivatives computed in this method can be used to calculate an approximation of the covariance of the estimates $\boldsymbol{\theta}$. This approximation indicates the confidence which can be placed in the estimates of the rigid motions. Section 6 describes the Lagrange/Newton approach for minimising Eq. (4), while Sect. 7 presents the motion covariance calculation.

A significant difference between the motion estimates obtained from Eq. (4) and previously proposed techniques, is the estimation of not only the rigid motions, but also the *estimation of the true positions of the corresponding points*. In Eq. (4), the residuals are defined as the difference between each measured point and its estimated position. This contrasts with previous formulations, which define the residuals as the distance between corresponding points once transformed into the world coordinate system. In these approaches the unconstrained, *unweighted* LSQ formulation for determining the maximum likelihood estimate $\hat{\boldsymbol{\theta}}$ is:

Find $\hat{\boldsymbol{\theta}}$ which minimises

$$\Theta(\hat{\boldsymbol{\theta}}) = \sum_{\mu=1}^{P}\sum_{i=1}^{N_\mu} \left\| \hat{\boldsymbol{f}}^{\alpha} \star \boldsymbol{p}_i^\alpha - \hat{\boldsymbol{f}}^{\beta} \star \boldsymbol{p}_i^\beta \right\|^2 \quad (5)$$

However, the estimates obtained by minimising Eq. (5) are only optimal for isotropic, identically, independent, normally distributed measurement errors. The experimental results in Sect. 8 illustrate the increased accuracy of the estimates $\hat{\boldsymbol{\theta}}$ obtained from Eq. (4) over those obtained from Eq. (5).

6. Solving the Minimisation Problem

To solve the constrained minimisation problem Eq. (4), the method of Lagrange multipliers is used. The extended objective function

$$\boldsymbol{\Gamma}(\hat{\boldsymbol{W}}, \hat{\boldsymbol{\theta}}, \boldsymbol{\lambda}) = \Phi(\hat{\boldsymbol{W}}) + \boldsymbol{\lambda}^\top \boldsymbol{G}(\hat{\boldsymbol{W}}, \hat{\boldsymbol{\theta}}) \quad (6)$$

is minimised with respect to $\hat{\boldsymbol{W}}$, $\hat{\boldsymbol{\theta}}$ and $\boldsymbol{\lambda}$. This nonlinear function must be minimised using an iterative numerical technique. A Newton method, where the function $\boldsymbol{\Gamma}(\hat{\boldsymbol{W}}, \hat{\boldsymbol{\theta}}, \boldsymbol{\lambda})$ is linearised with respect to $\hat{\boldsymbol{W}}$ and $\hat{\boldsymbol{\theta}}$, is used to obtain incremental updates $\Delta\hat{\boldsymbol{w}}$ and $\Delta\hat{\boldsymbol{\theta}}$, and the parameters values at each step are assigned as

$$\hat{\boldsymbol{w}}_{i(k+1)}^\mu = \hat{\boldsymbol{w}}_{i(k)}^\mu + \Delta\hat{\boldsymbol{w}}_{i(k)}^\mu \quad (7)$$

$$\hat{\boldsymbol{\theta}}_{k+1} = \hat{\boldsymbol{\theta}}_k + \Delta\hat{\boldsymbol{\theta}}_k \quad (8)$$

where k represents the iteration number.

The details of the derivation are omitted, and only the expressions for $\Delta\hat{\boldsymbol{w}}$ and $\Delta\hat{\boldsymbol{\theta}}$ are presented. The interested reader is referred to [3] p.155 for a detailed description of the derivation.

Some useful quantities, which come from the Taylor series expansion of $\boldsymbol{\Gamma}(\hat{\boldsymbol{W}}, \hat{\boldsymbol{\theta}}, \boldsymbol{\lambda})$, are first defined:

$$\boldsymbol{e}_i^\mu = \hat{\boldsymbol{w}}_i^\mu - \boldsymbol{w}_i^\mu \quad (9)$$

$$\boldsymbol{A}_i^\mu \equiv \partial \boldsymbol{g}_i^\mu / \partial \hat{\boldsymbol{W}}_i^\mu = \begin{bmatrix} \boldsymbol{R}^\alpha & -\boldsymbol{R}^\beta \end{bmatrix} \quad (10)$$

$$\boldsymbol{B}_i^\mu \equiv \partial \boldsymbol{g}_i^\mu / \partial \boldsymbol{\theta} = \left[\cdots \quad \frac{\partial \boldsymbol{f}^\alpha \star \boldsymbol{p}_i^\alpha}{\partial \boldsymbol{f}^\alpha} \quad \cdots \quad -\frac{\partial \boldsymbol{f}^\beta \star \boldsymbol{p}_i^\beta}{\partial \boldsymbol{f}^\beta} \quad \cdots \right] \quad (11)$$

$$\boldsymbol{C}_i^\mu = \boldsymbol{A}_i^\mu \boldsymbol{V}_i^\mu \boldsymbol{A}_i^{\mu\top} \quad (12)$$

$$\boldsymbol{D} = \sum_{\mu=1}^{P}\sum_{i=1}^{N_\mu} \boldsymbol{B}_i^{\mu\top} \boldsymbol{C}_i^{\mu-1} \boldsymbol{B}_i^\mu \quad (13)$$

where $\boldsymbol{R}^\alpha$ and $\boldsymbol{R}^\beta$ are the rotation matrices formed from the rotational components of $\boldsymbol{f}^\alpha$ and $\boldsymbol{f}^\beta$, respectively.

The new parameter and point estimates are then updated according to Eq. (7) and Eq. (8) using the following expressions for the increments:

$$\Delta\hat{\boldsymbol{\theta}} = \boldsymbol{D}^{-1} \sum_{\mu=1}^{P}\sum_{i=1}^{N_\mu} \boldsymbol{B}_i^{\mu\top} \boldsymbol{C}_i^{\mu-1} (\boldsymbol{A}_i^\mu \boldsymbol{e}_i^\mu - \boldsymbol{g}_i^\mu) \quad (14)$$

$$\boldsymbol{\lambda}_i^\mu = \boldsymbol{C}_i^{\mu-1} (\boldsymbol{B}_i^\mu \Delta\hat{\boldsymbol{\theta}} - \boldsymbol{A}_i^\mu \boldsymbol{e}_i^\mu + \boldsymbol{g}_i^\mu) \quad (15)$$

$$\Delta\hat{\boldsymbol{w}}_i^\mu = -\boldsymbol{e}_i^\mu - \boldsymbol{V}_i^\mu \boldsymbol{A}_i^{\mu\top} \boldsymbol{\lambda}_i^\mu \quad (16)$$

For clarity the iteration index k has been omitted, but should be considered implicit in Eqs. (9)–(16) since they are recomputed for each iteration.

The system as described has a global degeneracy – the application of the same rigid motion to all point sets results in no change to the cost function. For this reason, we must impose the condition that one of the motions is fixed (generally to the identity transformation). In the computation of $\Delta\hat{\boldsymbol{\theta}}$ etc., this is achieved by substituting $\boldsymbol{B} = \breve{\boldsymbol{B}}$ in Eqs. (14)–(16), where $\breve{\boldsymbol{B}}$ is the matrix $\boldsymbol{B}$ deprived of the 6 columns which correspond to the chosen fixed view (refer to Eq. (11)). The choice of fixed view is unimportant, and has no influence on the solution. In this work the first view, $\alpha = 1$, was chosen.

7. Motion Estimate Uncertainty

Following the estimation of the rigid motions, we wish to obtain a measure of the uncertainty in those estimates. Using the method of the previous section, this uncertainty can be expressed in the form of an error covariance matrix.

Before proceeding with the derivation, we make the following definitions:

$$\boldsymbol{A} = \begin{bmatrix} \boldsymbol{A}_1^1 & \dots & \boldsymbol{0} \\ \vdots & \ddots & \vdots \\ \boldsymbol{0} & \dots & \boldsymbol{A}_{N_P}^P \end{bmatrix}$$

and similarly for $\boldsymbol{C}$ w.r.t. $\boldsymbol{C}_i^\mu$ and $\boldsymbol{V}$ w.r.t. $\boldsymbol{V}_i^\mu$. Also

$$\boldsymbol{B} = \begin{bmatrix} \boldsymbol{B}_1^{1\top} & \dots & \boldsymbol{B}_{N_P}^{P\top} \end{bmatrix}^\top$$

and similarly for $\boldsymbol{E}$. The matrices $\boldsymbol{G}$ and $\boldsymbol{W}$ are as defined in Sect. 5. The double sums over μ and i from Eq. (14) are now replaced by

$$\Delta\hat{\boldsymbol{\theta}} = \boldsymbol{D}^{-1}\boldsymbol{B}^\top\boldsymbol{C}^{-1}(\boldsymbol{A}\boldsymbol{E} - \boldsymbol{G}) \tag{17}$$

Since, at the minimising solution, the constraint $\boldsymbol{G} = \boldsymbol{0}$ is satisfied, the change $\delta\hat{\boldsymbol{\theta}}$ in $\hat{\boldsymbol{\theta}}$ due to a small change $\delta\boldsymbol{W}$ in $\boldsymbol{W}$ is approximated by

$$\delta\hat{\boldsymbol{\theta}} \approx \boldsymbol{D}^{-1}\boldsymbol{B}^\top\boldsymbol{C}^{-1}\boldsymbol{A}\delta\boldsymbol{E} \tag{18}$$

where $\delta\boldsymbol{E} = (\partial\boldsymbol{E}/\partial\boldsymbol{W})\delta\boldsymbol{W} = -\delta\boldsymbol{W}$. Setting $\boldsymbol{V}_W = E[\delta\boldsymbol{W}\ \delta\boldsymbol{W}^\top]$ we have

$$\begin{aligned}\boldsymbol{V}_\theta &\equiv E[\delta\hat{\boldsymbol{\theta}}\ \delta\hat{\boldsymbol{\theta}}^\top] \\ &\approx \boldsymbol{D}^{-1}\boldsymbol{B}^\top\boldsymbol{C}^{-1}\boldsymbol{A}\boldsymbol{V}_W\boldsymbol{A}^\top\boldsymbol{C}^{-1}\boldsymbol{B}\boldsymbol{D}^{-1}\end{aligned} \tag{19}$$

The covariance $\boldsymbol{V}_W$ can be approximated by $\boldsymbol{V}$ (as defined previously). Since $\boldsymbol{C} = \boldsymbol{A}\boldsymbol{V}\boldsymbol{A}^\top$ and $\boldsymbol{D} = \boldsymbol{B}^\top\boldsymbol{C}^{-1}\boldsymbol{B}$, the error covariance $\boldsymbol{V}_\theta$ can be approximated by

$$\begin{aligned}\boldsymbol{V}_\theta &\approx \boldsymbol{D}^{-1}\boldsymbol{B}^\top\boldsymbol{C}^{-1}\boldsymbol{B}\boldsymbol{D}^{-1} \\ &= \boldsymbol{D}^{-1}\end{aligned} \tag{20}$$

From this equation, it can be seen that the error covariance matrix $\boldsymbol{V}_\theta$ of the motion parameter estimate is approximated by $\boldsymbol{D}^{-1}$. Error covariance matrices for individual motions are obtained by extracting the appropriate 6×6 sub-matrices from around the diagonal of $\boldsymbol{V}_\theta$. The registration parameter estimates can now be treated as probabilistic motions (see [21]).

8. Experimental Results

Before describing the experimental tests and results, some practicalities, concerning the Newton iterative technique for minimising the residual functions in Eq. (4) and Eq. (5), are discussed.

Initial estimates: All of the experiments utilised an unweighted, direct pairwise method to generate initial estimates, which were then refined using the proposed algorithm.

Stopping criterion: The estimation process is terminated when the (normalised) change in transform estimates from one Newton iteration to the next is less than 10^{-6}.

Experimental tests were conducted with both synthetic and real data. We describe each separately below.

8.1 Synthetic Data

In the first set of tests, object points were chosen randomly within a $10 \times 10 \times 10$ cube with "diagonally opposite" corners at world coordinates $(5, 5, 5)$ and $(-5, -5, 15)$. A single three sensor configuration, was used in each of the experiments. Results were obtained for two values of error eccentricities and a range of signal to noise ratios (SNR). Two different numbers (10 and 20) of corresponding points per correspondence set were tested. The point measurement error covariance for each sensor were joint normally distributed, with diagonal covariance matrices $\mathrm{diag}(\boldsymbol{\Sigma}_{i,\mu}^{\alpha(\mu)}) = \mathrm{diag}(\boldsymbol{\Sigma}_{i,\mu}^{\beta(\mu)}) = (\sigma_\mathrm{a}^2, \sigma_\mathrm{a}^2, \sigma_\mathrm{r}^2)^\top$. The error eccentricity values were $e = 0$ (isotropic), $e = 0.87$, and $e = 0.97$, where $e = \sqrt{\sigma_\mathrm{r}^2 - \sigma_\mathrm{a}^2}/\sigma_\mathrm{r}$.

The registration parameter estimates for $\hat{\boldsymbol{\theta}}$ were calculated using both the proposed WLSQ algorithm, and also an unweighted LSQ in which the algorithm has no prior knowledge of the point error distribution (isotropic assumption). This allows assessment of improvements achievable through error modeling. Each experiment was repeated 100 times in a Monte Carlo fashion.

In a manner similar to [14], registration performance is measured by the RMS (root mean square) rotation angle error in the calculated registration parameters. As expected, the results obtained under isotropic noise were identical for both methods, and we omit those results in the interests of brevity. Figure 3 presents plots of RMS rotational error versus SNR for the three view case using the two non–isotropic error models. Results from the proposed (error modeled) technique are marked with '$\circ$,' and the "unmodeled" results with '$\times$.'

From these results we make the following observations: (1) the algorithm is capable of excellent registration accuracy (less than 0.15 radian rotation angle error at 10 dB SNR), (2) registration accuracy improves with increasing number of points per correspondence set, (3) registration accuracy is improved by modeling sensor error characteristics, (4) the use of error models maintains nearly constant error performance with increasing error eccentricity, while the isotropic assumption causes

performance degradation, and (5) the relative accuracy improvement from error modeling increases with the error model eccentricity, and decreases with the number of point pairs and views.

A separate experiment, involving a six sensor configuration, was performed to compare the approximated error covariance, $\boldsymbol{V}_\theta \approx \boldsymbol{D}^{-1}$, with the experimental covariance obtained from Monte Carlo trials. Table 1 shows the standard deviations of errors for two of the six views in the experiment, comparing the approximated and experimental error standard deviations (computed as the square root of the diagonal elements of the error covariance matrices). It can be seen that the approximated error standard deviations estimate the experimental values to within approximately ±5%. Similar results were obtained for the other views in the experiment. We consider this to be an excellent result, since according to Bard ([3], p.179), theoretical estimates of $\mathbf{V}_\theta$ are generally only expected to be within one order of magnitude of the experimental values.

8.2 Real Data

The experiments just described assume the existence of correspondence information. To demonstrate the use of the proposed technique with real data, we have integrated the algorithm into a generalised multiview surface registration system based upon the Iterative Closest Point (ICP) algorithm, proposed by Besl and McKay [6]. The principle of the ICP is to first assume that the partial surface views are already in approximate alignment. Each point in one view is matched with the closest point in the other view, thus forming correspondences. Following the matching process, the rigid transformation is computed which minimises the distance between corresponding point pairs (point set registration). The process is repeated until convergence.

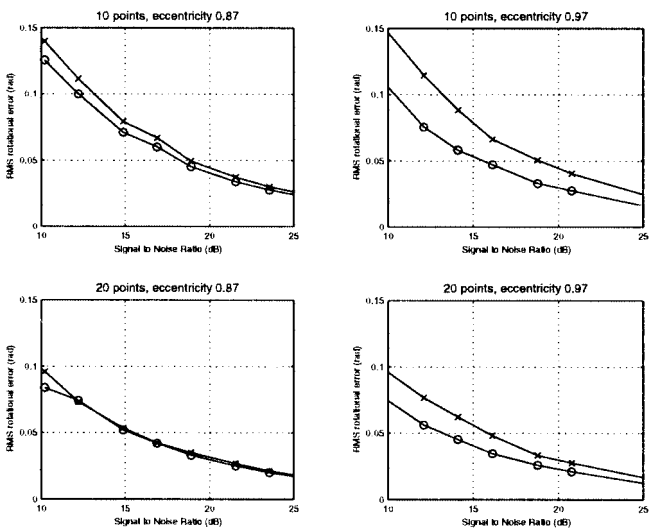

Fig. 3 Comparison results for three view configuration. ∘ – error models, × – no error models.

Table 1 Theoretical and experimental standard deviations of errors in motion parameters for two different views $\boldsymbol{f}^3$ and $\boldsymbol{f}^5$ (multiplied by 1000 for display).

Source	$\sigma_{r_1^3}$	$\sigma_{r_2^3}$	$\sigma_{r_3^3}$	$\sigma_{t_1^3}$	$\sigma_{t_2^3}$	$\sigma_{t_3^3}$
Th.	0.653	0.779	1.04	6.73	6.93	10.1
Exp.	0.632	0.787	1.06	6.77	6.68	10.5
Source	$\sigma_{r_1^5}$	$\sigma_{r_2^5}$	$\sigma_{r_3^5}$	$\sigma_{t_1^5}$	$\sigma_{t_2^5}$	$\sigma_{t_3^5}$
Th.	0.550	0.686	0.600	7.19	5.99	9.96
Exp.	0.541	0.692	0.578	7.42	5.81	10.0

An implicit assumption in this approach is that one surface is a subset of the other, for example when matching measured data to a shape template. However, when registering partial surface views for object modeling, the views generally share a region of mutual overlap instead. In this case the subset assumption of the ICP causes significant problems, because there will be points in one view which have no corresponding point in the other, yet will still be "forced" to match. The false correspondences thus produced negatively influence the registration result.

A number of heuristic constraints were proposed to overcome this problem, including:

- *maximum match distance*, where matched points are rejected if they are greater than a threshold distance from each other (e.g. [33]),
- *normal vector compatibility*, where matched points are discarded if their normal vectors diverge by greater than a threshold angle [13], and
- *boundary match rejection*, whereby matches are prevented between points whose closest corresponding point is on the boundary of the other surface [30].

The ICP was originally devised to match just one surface to another, i.e. pairwise surface matching, however it is easily generalised to the multiple view case, simply by matching each point with the closest point in all other overlapping views (e.g. [5]). In producing the following results, initial ICP iterations were performed with a fast, non error-modeling multiview point registration method [32]. Once convergence was obtained, the last few iterations were completed using our proposed error modeling technique.

The data chosen for this example was a set of 14 high resolution range images of a wooden model duck, courtesy of the Visual Information Technology Group at the Research Council of Canada. The data were resampled to a resolution of approximately 0.6 mm in the XY scanning plane. Several of these views are shown in Fig. 4.

No sensor error model information was available for this data set, instead a generic model was employed in which the X and Y variance was equal to the square of the sampling resolution, and the Z variance set to

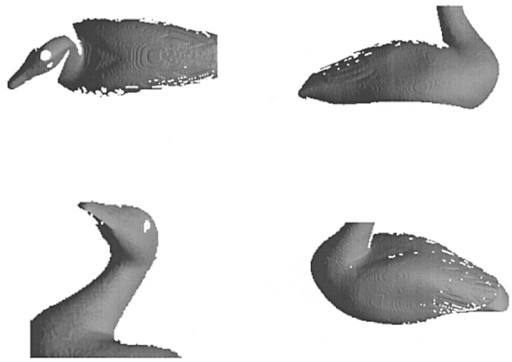

Fig. 4 Sample of input range images.

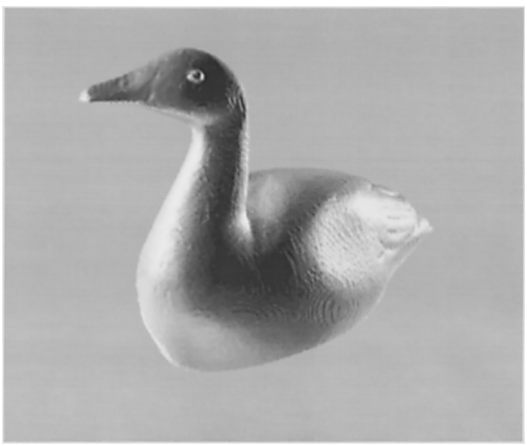

Fig. 5 Registered views.

Table 2 Rotation and translation error standard deviations for the duck data set.

View No.	2	6	10	14
σ_r (milliradians)	0.029	0.023	0.023	0.027
σ_t (μm)	2.070	1.905	1.914	2.378

10 times that. Thus $\sigma_x^2 = \sigma_y^2 = 0.36$ and $\sigma_z^2 = 3.6\,\mathrm{mm}^2$ in each local coordinate system.

The modified ICP algorithm described above was applied to the data, the results of which are shown in Fig. 5. From visual inspection the quality of the registration is clear. The registration uncertainty information arising from this registration problem is a 78×78 covariance matrix, representing the error covariances of 6 parameters for 13 views. The first view, being locked to the canonical coordinate system, has no uncertainty information.

The method of Kanazawa and Kanatani [17] was used to convert this detailed covariance data into a primary deviation pair, which represents a one-σ confidence interval for each parameter. To more clearly indicate the registration uncertainty, we used the primary deviation pairs to compute standard deviations of rotation error angles and translation distances. Table 2 shows these results for a selection of the views.

The results in Table 2 show that a very high degree of registration accuracy has been achieved, with an average rotation error of approximately 0.025×10^{-3} radians, and translational errors of approximately 2×10^{-6} meters. This translational error is significantly smaller than the error on individual points, which is expected due to the very large number of matched points (approx. 90,000).

9. Conclusion

Our review of 3D registration literature identified the absence of methods which are capable of optimally and globally registering multiple correpondence sets, where the points in these sets are subject to heteroscedastic, anisotropic, measurement errors.

We have formulated the global point set registration task as a constrained, weighted, least squares estimation problem. In particular, the formulation utilises (2nd order) statistical sensor noise models. The performance of the WLSQ registration method was compared numerically with an unweighted LSQ method which assumes an isotropic error model. The results illustrated that registration accuracy is improved by error modeling. The degree of improvement is related to the error model eccentricity, and the number of corresponding point pairs, as described in the previous section.

The proposed technique was then incorporated into a multiple view ICP-type surface registration system, and used to compute the resulting registration accuracy. The uncertainty in rotation and translation estimates was found to be very small, mainly due to the very large number of point correspondences.

We conclude that error modeling (and the proposed WLSQ registration technique) are of greatest value when registering sets containing small numbers of points, obtained from sensors whose error distributions are significantly anisotropic. This should particularly suit sparse, feature-based correspondence selection methods. Otherwise, registration accuracy improvements are still obtained however the effect is less dramatic.

References

[1] K.S. Arun, T.S. Huang, and S.D. Blostein, "Least-squares fitting of two 3-D point sets," IEEE Trans. Pattern Anal. & Mach. Intell., vol.PAMI-9, no.5, pp.698–700, Sept. 1987.
[2] N. Ayache, Artificial Vision for Mobile Robots, MIT Press, 1991.
[3] Y. Bard, Nonlinear Parameter Estimation, Academic Press, New York, USA, 1974.
[4] R. Benjemaa and F. Schmitt, "A solution for the registration of multiple 3D point sets using unit quaternions," Proc. ECCV '98, pp.34–50, Freiburg, Germany, June 1998.
[5] R. Bergevin, M. Soucy, H. Gagnon, and D. Larendeau, "Towards a general multi-view registration technique," IEEE Trans. Pattern Anal. & Mach. Intell., vol.18, no.5, pp.540–547, May 1996.

[6] P.J. Besl and N.D. McKay, "A method of registration of 3-D shapes," IEEE Trans. Pattern Anal. & Mach. Intell., vol.14, no.2, pp.239–256, Feb. 1992.
[7] J.A.R. Blais, "Three-dimensional similarity," The Canadian Surveyor, vol.1, pp.71–76, 1972.
[8] P. Boulanger, V. Moron, and T. Redarce, "High-speed and non-contact validation of rapid prototyping parts," Proc. SPIE Rapid Product Development Technologies, pp.46–60, June 1996.
[9] C. Dorai, J. Weng, and A.K. Jain, "Optimal registration of object views using range data," IEEE Trans. Pattern Anal. & Mach. Intell., vol.19, no.10, Oct. 1997.
[10] C. Eckart and G. Young, "The approximation of one matrix by another of lower rank," Psychometrika, vol.1, pp.211–218, 1936.
[11] D.W. Eggert, A.W. Fitzgibbon, and R.B. Fisher, "Simultaneous registration of multiple range views for use in reverse engineering of CAD models," Computer Vision and Image Understanding, vol.69, no.3, pp.253–272, March 1998.
[12] D.W. Eggert, A. Lorusso, and R.B. Fisher, "Estimating 3-D rigid body transformations: A comparison of four major algorithms," Machine Vision and Applications, vol.9, pp.272–290, 1997.
[13] G. Godin, M. Rioux, and R. Baribeau, "Three-dimensional registration using range and intensity information," Proc. SPIE, vol.2350: Videometrics III, pp.279–290, 1994.
[14] R.M. Haralick, H. Joo, C.N. Lee, X. Zhuang, V.G. Vaidya, and M.B. Kim, "Pose estimation from corresponding point data," IEEE Trans. Syst., Man. & Cybern., vol.19, no.6, pp.1426–1446, 1989.
[15] B.K.P. Horn, "Close-form solution of absolute orientation using unit quaternions," J. Opt. Soc. Am. A, vol.4, no.4, pp.629–642, April 1987.
[16] B.K.P. Horn, H.M. Hilden, and S. Negahdaripour, "Close-form solution of absolute orientation using orthonormal matrices," J. Opt. Soc. Am. A, vol.5, no.7, pp.1127–1135, July 1988.
[17] Y. Kanazawa and K. Kanitani, "Reliability of 3D reconstruction by stereo vision," IEICE Trans. Inf. & Syst., vol.E78-D, no.10, pp.1301–1306, Oct. 1995.
[18] B. Matei and P. Meer, "Optimal rigid motion estimation and performance evaluation with bootstrap," Proc. IEEE Conf. on Computer Vision and Pattern Recognition (CVPR '99), vol.I, pp.339–345, June 1999.
[19] P. Meer, D. Mintz, A. Rosenfeld, and D.Y. Kim, "Robust regression methods for computer vision: A review," Int. J. Computer Vision, vol.6, no.1, pp.59–70, 1991.
[20] N. Ohta and K. Kanatani, "Optimal estimation of three-dimensional rotation and reliability evaluation," B. Neumann and H. Burkhardt, eds., Computer Vision - ECCV '98, vol.1, pp.175–187, Springer, June 1998.
[21] X. Pennec and J.P. Thirion, "Validation of 3-D registration methods based on points and frames," Proc. 5th Int. Conf. on Computer Vision (ICCV '95), pp.557–562, IEEE Comp. Soc. Press, 1995.
[22] X. Pennec and J.P. Thirion, "A framework for uncertainty and validation of 3-D registration methods based on points and frames," Int. J. Computer Vision, vol.25, no.3, pp.203–229, 1997.
[23] F. Sanso, "An exact solution of the roto-translation problem," Photogrammetria, vol.29, pp.203–216, 1973.
[24] P.H. Schönemann, "A generalized solution of the orthogonal procrustes problem," Psychometrika, vol.31, pp.1–10, 1966.
[25] G.H. Schut, "On exact linear equations for the computation of rotational element of absolute orientation," Photogrammetria, vol.15, no.1, pp.34–37, 1960.
[26] H.-Y. Shum, K. Ikeuchi, and R. Reddy, "Principal component analyis with missing data and its application to polyhedral object modeling," IEEE Trans. Pattern Anal. & Mach. Intell., vol.17, no.9, Sept. 1995.
[27] A.J. Stoddart and A. Hilton, "Registration of multiple point sets," Proc. IEEE Int. Conf. on Pattern Recognition (ICPR '96), vol.A, pp.40–44, Vienna, Austria, Aug. 1996.
[28] E.H. Thompson, "An exact linear solution of the problem of absolute orientation," Photogrammetria, vol.15, no.4, pp.163–178, 1958.
[29] M. Tienstra, Calculation of Orthogonal Matrices, ITC, Delft, 1969.
[30] G. Turk and M. Levoy, "Zippered polygon meshes from range images," Computer Graphics Proc., SIGGRAPH 94, pp.311–318, ACM Press, July 1994.
[31] J. Williams and M. Bennamoun, "Multiple view 3D registration using statistical error models," Proc. Vision Modelling and Visualisation '99, Erlangen, pp.83–90, Germany, Nov. 1999.
[32] J. Williams and M. Bennamoun, "Simultaneous registration of multiple point sets using orthonormal matrices," Proc. IEEE Int. Conf. on Acoustics, Speech & Signal Processing (ICASSP 2000), vol.IV, pp.2199–2202, Istanbul, Turkey, June 2000.
[33] Z. Zhang, "Iterative point matching for registration of free-form curves and surfaces," Int. J. Computer Vision, vol.13, no.2, pp.119–152, 1994.
[34] X.H. Zhuang and Y. Huang, "Robust 3D pose estimation," IEEE Trans. Pattern Anal. & Mach. Intell., vol.16, no.8, pp.818–824, 1994.

John Williams is currently in the third year of his Ph.D. at the Queensland University of Technology (QUT) in Brisbane, Australia. His research investigates 3D surface registration and reconstruction and, in particular, quantifying the effects of measurement noise on these processes.

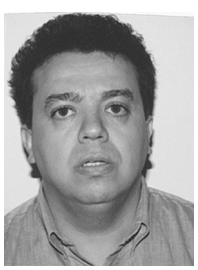

Mohammed Bennamoun finished his Masters of Science (M.Sc.) degree by research in Control Theory at Queen's University, Canada, and Ph.D. from Queensland University of Technology (QUT), Australia. He is currently the Director the Space Centre for Satellite Navigation, School of Electrical & Electronics Systems Engineering at QUT. He has participated in the organisation of many conferences including IEEE TENCON '97. His areas of interest include: Control Theory, Robotics, Obstacle avoidance, Object Recognition, Artificial Neural Networks, and Signal Processing.